

# ICA-based Individualized Differential Structure Similarity Networks for Predicting Symptom Scores in Adolescents with Major Depressive Disorder

Xiang Li, Ming Xu, Rongtao Jiang, Xuemei Li, Vince D. Calhoun, *Fellow, IEEE*, Xinyu Zhou, and Jing Sui\*, *Senior Member, IEEE*

**Abstract**—Major depressive disorder (MDD) is a complex mood disorder characterized by persistent and overwhelming depression. Previous studies have identified large scale structural brain alterations in MDD, yet most are group analyses with atlas-parcellated anatomical regions. Here we proposed a method to measure individual difference by independent component analysis (ICA)-based individual difference structural similarity network (IDSSN). This approach provided a data-adaptive, atlas-free solution that can be applied to new individual subjects. Specifically, we constructed individualized whole-brain structural covariance networks based on network perturbation approach using spatially constrained ICA. First, a set of benchmark independent components (ICs) were generated using gray matter volume (GMV) from all healthy controls. Then individual heterogeneity was obtained by calculating differences and other similarity metrics between ICs derived from “each one patient + all controls” and the benchmark ICs, resulting in 32 imaging features and structural similarity networks for each patient, which can be used for predicting multiple clinical symptoms. We estimated IDSSN for 189 adolescent MDD patients aged 10-20 years and compared them to 112 healthy adolescents. We tested their predictability of the Hamilton Anxiety Scale, the 17-item Hamilton Depression Scale and six clinical syndromes using connectome-based predictive modeling. The prediction results showed that ICA-based IDSSN features reveal more disease-specific information than those using other brain templates. We also found that depression-associated networks mainly involved the default-mode network and visual network. In conclusion, our study proposed an adaptive method that improves the ability to detect GMV deviations and specificity between one individual patient and healthy groups, providing a new perspectives and insights for evaluating individual-level clinical heterogeneity based on brain structures.

## I. INTRODUCTION

Major depressive disorder (MDD), a serious mental disorder, is characterized by persistent depressed mood and decreased interest, and often accompanied by cognitive impairment and various physical complaints[1]. Although tremendous efforts have been dedicated to understanding the mechanisms by which MDD arises and to seeking effective therapies. However, much remains unknown about the etiology and pathogenesis of the disorder. The early stages of individual development are known to be an important time for

the development of brain structure and function. As one of the most common psychiatric disorders during childhood and adolescence, MDD can have a significant impact when it develops during childhood and adolescence. Poor performance in school, increased risk for other mental health disorders, and substance use disorders have all been associated with a diagnosis of MDD in childhood[1]. Therefore, early detection and research on MDD in childhood and adolescence is of great importance.

With the help of magnetic resonance imaging (MRI), the structural brain abnormalities in MDD have been widely reported [2, 3]. However, most previous studies have focused on brain alterations in isolated anatomical regions and ignored potential associations between brain regions. Given that the brain is known to be a complex network, assessing the connections between different anatomical regions associated with the disorder can provide new insights into MDD psychopathology.

Brain structural covariance networks describe morphological features of brain regions, such as gray matter volume, based on common variation at the group level, and demonstrate modular structure with overlap between functional regions[4]. Considering normative modeling has recently emerged as a promising statistical method for mapping heterogeneity of imaging features at the individual level, which can provide statistical inferences about the extent to which each individual deviates from normal patterns. Therefore, the construction of individual-level structural covariance networks holds great promise for revealing individual differences in morphological covariance between regions. Importantly, normative modeling has been successfully applied to quantify structural heterogeneity at the individual level in schizophrenia, attention-deficit/hyperactivity disorder, and autism.

Existing studies constructing individualized structural covariance networks have been primarily relied on pre-defined brain atlas[5]. Using different brain parcellation schemes would produce different results. So far, there is no method to construct individualized structural covariance networks without discussing brain parcellation schemes. Therefore, we construct independent component analysis-based (ICA-based instead of atlas-based) individual difference structural

Xiang Li and Ming Xu are with the National Laboratory of Pattern Recognition, Institute of Automation, Chinese Academy of Sciences, Beijing, China, and School of Artificial Intelligence, University of Chinese Academy of Sciences, Beijing, China.

Rongtao Jiang is with the Department of Radiology and Biomedical Imaging, Yale School of Medicine, CT, United States.

Xinyu Zhou (email: [zhouxinyu@cqmu.edu.cn](mailto:zhouxinyu@cqmu.edu.cn)) and Xuemei Li are with the Department of Psychiatry, The First Affiliated Hospital of Chongqing Medical University, Chongqing, China.

Vince D Calhoun and Jing Sui are with the Tri-Institutional Centre for Translational Research in Neuroimaging and Data Science (TReNDS), Georgia State University Georgia Institute of Technology, and Emory University, Atlanta, GA, United States

Jing Sui is with the IDG/McGovern Institute for Brain Research, State Key Laboratory of Cognitive Neuroscience and Learning, Beijing Normal University, Beijing, China (corresponding author: [kittysj@gmail.com](mailto:kittysj@gmail.com)).

similarity networks using the normative modeling approach. We explore the heterogeneity of structural similarity networks at the individual level using regional similarity networks[6], a novel morphological covariance network with high robustness, stability, and biological basis. We expect to provide new perspectives for understanding the neurobiological basis of MDD in children and adolescents.

In this study, using gray matter volume (GMV) extracted from sMRI, we constructed an ICA-based individual difference structural similarity network (IDSSN) based on 112 healthy controls (HCs) for 189 adolescents aged 10 to 20 years with MDD. We used connectome-based predictive modeling (CPM) to investigate the correlation between structural similarity networks and symptom manifestations of depression and anxiety [7].

## II. MATERIALS AND METHODS

### A. Participant Recruitment and Assessment

Adolescents with MDD ( $n = 210$ , including 122 drug-naïve participants and 80 medicated participants) and HCs ( $n = 117$ ) were recruited from the First Affiliated Hospital of Chongqing Medical University, Chongqing, China, through local media advertising. All procedures were approved by the Ethics Committee of Chongqing Medical University (approval ID: 2020-864), and all participants provided the written informed consent.

The 17-item Hamilton Depression Scale (HAMD-17) was used to evaluate the severity of depression in individuals with MDD, which included total scores and six syndrome scores related to somatization (HAMD 10, 11, 12, 15, 17), weight change (HAMD 16), cognitive disturbance (HAMD 2, 3, 9), Psycho-retardation (HAMD 1, 7, 8, 14), sleep disturbance (HAMD 4, 5, 6) and HAMD-6 (HAMD 1, 2, 7, 8, 10, 13) [8]. The Hamilton Anxiety Scale (HAMA) was used to evaluate anxiety severity.

TABLE I. A SUMMARY OF THE DEMOGRAPHIC INFORMATION

|                        | MDD (N=189)    | HC (N=112)     | P values   |
|------------------------|----------------|----------------|------------|
| Age (years)            | 15.54 ± 1.64   | 14.64 ± 2.67   | 7.0e-5***  |
| Sex (female/male)      | 51/138         | 47/65          | 1.1e-2*    |
| TIV (cm <sup>3</sup> ) | 1444.8 ± 138.9 | 1486.9 ± 118.3 | 7.7e-3**   |
| HAMD-17                | 18.26 ± 5.68   | 1.22 ± 1.47    | 8.0e-96*** |
| HAMA                   | 15.53 ± 6.74   | 1.70 ± 2.10    | 5.9e-65*** |
| Somatization           | 4.68 ± 1.90    | 0.43 ± 0.74    | 6.6e-67*** |
| Weight change          | 0.39 ± 0.68    | 0.07 ± 0.35    | 5.4e-6***  |
| Cognitive disturbance  | 4.55 ± 2.21    | 0.19 ± 0.45    | 1.9e-59*** |
| Psycho-retardation     | 5.02 ± 1.92    | 0.28 ± 0.66    | 4.8e-76*** |
| Sleep disturbance      | 2.68 ± 1.79    | 0.20 ± 0.49    | 1.5e-35*** |
| HAMD-6                 | 8.49 ± 3.03    | 0.62 ± 1.02    | 1.8e-80*** |

Data were presented as means ± standard deviation, except for gender was presented as the number of people. Anxiety/somatization: HAMD 10, 11, 12, 15, 17; Weight change: HAMD 16; Cognitive disturbance: HAMD 2, 3, 9; Psychomotor retardation: HAMD 1, 7, 8, 14; Sleep disturbance: HAMD 4, 5, 6; HAMD-6: HAMD 1, 2, 7, 8, 10, 13. MDD major depressive disorder, HCs health controls, HAMD-17 Hamilton depression scale-17, HAMA Hamilton anxiety scale, TIV total intracranial volume. \* $p < 0.05$ ; \*\*indicated  $p < 0.01$ ; \*\*\*indicated  $p < 0.001$ .

MDD patients were diagnosed through structured clinical interview for DSM-V depressive symptoms and satisfied following inclusion criteria: (1) HAMD-17 total scores  $> 7$ ; (2) first episode. HCs were required to have a HAMD-17 total score  $\leq 7$ . All participants were aged 10 to 20 years. Exclusion

criteria for all participants involve followings: (1) a history of other major psychiatry and neurological disorders; (2) a history of organic head trauma; (3) a history of substance abuse; (4) any conditions not suitable for MRI scanning.

Five participants were excluded due to inadequate signal in several brain regions. Therefore, 301 participants were retained (112 HCs and 189 MDD adolescents, including 109 drug-naïve participants and 80 medicated participants) for further analysis. Demographic and clinical features of the 189 MDD patients and 112 HCs are presented in Table I. The mean age, sex proportion, and total intracranial volume (TIV) were different from each other ( $p < 0.05$ ) between the MDD patients and HCs. Compared with HCs, MDD patients have significant higher severity in all eight clinical measures ( $p < 0.001$ ) (Table I).

### B. Image Acquisition and preprocessing

The high resolution T1-weighted (T1w) structural images were acquired using a Siemens Magnetom Skyra 3T scanner with a 32-channel head coil. Each participant was instructed to lie down and relax, to keep their eye closed and to stay awake and to avoid performing specific cognitive task. T1w structural images were acquired using magnetization-prepared rapid gradient-echo (MPRAGE) sequence with the following parameters: repetition time (TR) = 2000 ms, echo time (TE) = 2.56 ms, inversion time (TI) = 900 ms, flip angle = 9°, matrix size = 256 × 256, field of view (FOV) = 256 mm × 256 mm, slice thickness = 1 mm, slices per slab = 192, and voxel size was 1.0 mm × 1.0 mm × 1.0 mm.

T1 image data was pre-processed and analyzed using the CAT12 toolbox (<https://neuro-jena.github.io/cat/>) and the SPM12 software package (<https://www.fil.ion.ucl.ac.uk/spm/>). Specifically, the T1w images were firstly bias-corrected, and then segmented into gray matter (GM), white matter (WM), and cerebrospinal fluid (CSF). Next, all segmented images were spatially normalized to the standard Montreal Neurological Institute (MNI) space using the ICBM-152 template (East Asian) with a voxel size of 1.5 mm × 1.5 mm × 1.5 mm. Finally, the normalized segmentations were modulated by scaling with the amount of volume changes due to spatial registration, resulting in GMV images for each subject. GMV images were smoothed with commonly used smoothing kernels at full width at half maximum (FWHM) for subsequent analysis. Age, gender, and TIV were also estimated to correct for individual differences in brain size.

### C. Constructing the ICA-based IDSSN

Figure 1 summarizes the flowchart of constructing the ICA-based IDSSN. In the cohort of 189 MDD patients and 112 HCs, we used the spatial brain network template (NeuroMark\_fmri\_1.0 template available in the GIFT toolbox; <http://trendscenter.org/software/gift> and at <http://trendscenter.org/data>) as the reference to construct a benchmark independent component (IC) IC<sub>base</sub> covering the whole 112 HC subjects. By taking each HC's structural MRI data as input, the IC<sub>base</sub> spatially IC were computed by multi-objective optimized ICA with reference (MOO-ICAR), an approach that automatically and adaptively estimates baseline-level IC using the prior network

templates as guidance[9].

Computed by MOO-ICAR, 113 subjects [112 HCs and 1 MDD patient  $i$  ( $i=1, \dots, M$ )] were used to construct a new spatially IC, called disturbance IC ( $IC_{base+i}$ ). The difference between the disturbance IC and the baseline IC was calculated, i.e.,  $\Delta IC_i = IC_{base+i} - IC_{base}$ .  $\Delta IC_i$  represents the deviation of the GMV in the corresponding brain network spatial IC in patient  $i$  compared with the HCs. It can also ensure the independence of individual subjects' spatial IC and the correspondence between different subjects' components. Then, a total of 47 MRI imaging features were computed, including 14 intensity features and 33 texture features. Intensity features describe the distribution of voxel intensities within MRI images by commonly used basic metrics, such as mean and entropy. Texture features describe the pattern or spatial distribution of voxel intensities, such as contrast, homogeneity. We first normalized the features between different brain regions of an individual using the min-max method, and redundant features were defined as those that were highly correlated ( $r > 0.9$ ) with other features and 32 features were left for the subsequent analysis. Thus, a final feature matrix of  $53 \times 53$  structural similarity network (IDSSN) for each subject was obtained for further analysis[6]. Briefly, the IDSSN nodes were defined as the 53 ICs generated by MOO-ICAR, and the edge was calculated by computing Pearson's correlation using 32 features among different spatial ICs.

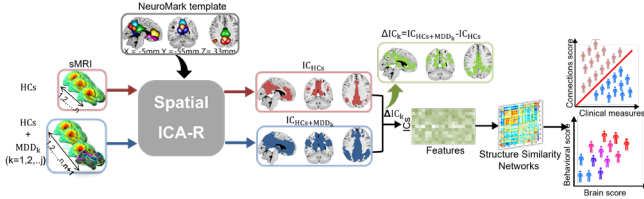


Figure 1. Flowchart describing the construction of the ICA-based individual difference structural similarity network (IDSSN)

#### D. The Prediction Performance of the ICA-based IDSSN

To evaluate the predictive performance of ICA-based IDSSN for symptom manifestations of depression and anxiety, and to determine the neurobiological basis of ICA-based IDSSN, we created a prediction model based on CPM with leave-one-out cross-validation (LOOCV) strategy. Edges that were positively correlated with clinical measures (HAMA, HAMD17 total scores and six syndrome scores) with a  $p < \text{positive threshold}$  (0.01) made up the positive network, in which positive network strength was calculated by summing values of all edges in positive network, and the same procedure was used to construct the negative network strength by edges that were negatively correlated with clinical measures. Positive and negative network strengths were utilized as imaging features to construct the prediction model. The process was repeated eight times using different clinical indicators (HAMA, HAMD total scores and six syndrome scores), so we ended up with eight prediction models with different parameters.

*Selecting predictive structure similarity networks:* Predictive consistent connections were determined by pulling together all features that appeared in all cross-validation loops in LOOCV. For better interpretation and visualization, we categorized edges into seven networks based on anatomical and functional properties, including subcortical network (SC), auditory network (AU), visual network (VI), sensorimotor network (SM), cognitive control network (CC), default-mode network (DM), and cerebellar network (CB). Next, we employed a calculation to index the relative contribution of each of the seven networks. That is, the contribution of edges was normalized for network size.

*Comparison of predictions based on different parcellation schemes or only on the extracted features:* To confirm the ability of the IDSSN method to extract individual-specific information, we 1) segmented GMV based on different brain atlases or segmentation schemes, such as anatomical automatic labeling (AAL) atlas which has 116 nodes, and NeuroMark template which have 53 nodes. Next, we used CPM to calculate the predictive ability of the obtained structural similarity network for eight clinical symptom scores. 2) using only the derived features as input into CPM to explore which feature better exploits individual-specific information.

We quantified model performance by calculating Spearman rank correlation between observed and predicted HAMA, HAMD total scores and six syndrome scores, and the coefficient of determination prediction  $R^2$ . We determined the significance of the model based on a  $p$ -value calculated from 5,000 permutation tests.

### III. RESULTS

Table II displays the prediction performances of depression and anxiety scores using structural similarity network constructed from ICA-based IDSSN, AAL atlas, and NeuroMark template. Notably, ICA-based IDSSN achieved better prediction accuracy for HAMD17 total scores ( $r_{[HAMD17]} = 0.51$ ,  $p = 2.8e-15$ ,  $R^2=0.24$  Figure 2a) and HAMA scores ( $r_{[HAMA]} = 0.46$ ,  $p = 2.7e-12$ ,  $R^2=0.25$ , Figure 2b) than using AAL atlas ( $r_{[HAMD17]} = 0.31$ ,  $p = 6.9e-6$ ,  $R^2=0.10$ ;  $r_{[HAMA]} = 0.15$ ,  $p = 3.5e-2$ ,  $R^2=0.01$ ) or NeuroMark template ( $r_{[HAMD17]} = 0.18$ ,  $p = 8.6e-3$ ,  $R^2=0.05$ ;  $r_{[HAMA]} = 0.27$ ,  $p = 8.7e-5$ ,  $R^2=0.07$ ). For the six syndrome scores of HAMD17, ICA-based IDSSN also achieved the best prediction performance (Table II). Likewise, we reran the pipeline using the derived features without calculating the structural similarity network to assess which feature is better to exploit the individual-specific information. The ICA-base method (MOO-ICAR) consistently performed the best in all prediction models ( $r_{[HAMD17]} = 0.37$ ,  $p = 4.8e-8$ ,  $R^2=0.13$ ,  $r_{[HAMA]} = 0.38$ ,  $p = 1.2e-8$ ,  $R^2=0.14$ ). However, the prediction accuracy is not as high as that of ICA-based IDSSN (Table III).

Several connections were identified in Figure 2c and Figure 2d. To prevent confusion, we removed the lower part of the cell plot in Figure 2c and Figure 2d. ICA-based IDSSN, which indicted edges' contributions and the number of edges for each macroscopic brain region. Macroscopic networks showed that more severe depression symptom was associated



with stronger connections between VI and SC, SM, CC and DM, and between AU and DM. Furthermore, milder depressive symptom was associated with stronger connectivity between DM and CC. In addition, macroscopic networks showed that worse anxiety symptom was associated with stronger connections within SM and within VI, between SM and AU, VI, and between AU and CC. Milder anxiety symptom was associated with stronger networks between SC and SM, VI, CC, between CC and SM, DM, between CB and AU, DM.

TABLE II. PREDICTION RESULTS USING **INDIVIDUAL STRUCTURAL SIMILARITY NETWORK FEATURES** BUILT BY AAL TEMPLATE, NEUROMARK TEMPLATE AND MOO-ICAR

|                    | AAL      |          |                       | NeuroMark |          |                       | ICA-based IDSSN (proposed) |          |                       |
|--------------------|----------|----------|-----------------------|-----------|----------|-----------------------|----------------------------|----------|-----------------------|
|                    | <i>r</i> | <i>p</i> | <i>R</i> <sup>2</sup> | <i>r</i>  | <i>p</i> | <i>R</i> <sup>2</sup> | <i>r</i>                   | <i>p</i> | <i>R</i> <sup>2</sup> |
| HAMD17             | 0.31     | 6.9e-6   | 0.10                  | 0.18      | 8.6e-3   | 0.05                  | <b>0.51</b>                | 2.8e-15  | 0.24                  |
| HAMA               | 0.15     | 3.5e-2   | 0.01                  | 0.27      | 8.7e-5   | 0.07                  | <b>0.46</b>                | 2.7e-12  | 0.25                  |
| Somatization       | 0.23     | 1.0e-3   | 0.02                  | 0.21      | 2.4e-3   | 0.06                  | 0.44                       | 5.2e-11  | 0.17                  |
| Weight change      | 0.31     | 4.5e-6   | 0.07                  | 0.28      | 5.8e-5   | 0.08                  | 0.40                       | 3.3e-9   | 0.15                  |
| cognitive disorder | 0.20     | 4.5e-3   | 0.03                  | 0.32      | 2.5e-6   | 0.07                  | 0.49                       | 1.1e-13  | 0.21                  |
| Psycho-retardation | 0.30     | 1.5e-5   | 0.03                  | 0.29      | 2.4e-5   | 0.09                  | 0.46                       | 4.5e-12  | 0.16                  |
| Sleep disorders    | 0.26     | 1.3e-4   | 0.05                  | 0.36      | 1.3e-7   | 0.07                  | 0.51                       | 3.9e-15  | 0.23                  |
| HAMD-6             | 0.27     | 9.4e-5   | 0.05                  | 0.30      | 1.0e-5   | 0.07                  | 0.52                       | 1.0e-15  | 0.26                  |

Anxiety/somatization: HAMD 10, 11, 12, 15, 17; Weight change: HAMD 16; Cognitive disturbance: HAMD 2, 3, 9; Psychomotor retardation: HAMD 1, 7, 8, 14; Sleep disturbance: HAMD 4, 5, 6; HAMD-6: HAMD 1, 2, 7, 8, 10, 13. MDD major depressive disorder, HCs health controls, HAMD-17 Hamilton depression scale-17, HAMA Hamilton anxiety scale. **Bold** values correspond to the highest correlation in HAMD17 and HAMA models.

TABLE III. PREDICTION RESULTS USING **ONLY DERIVED FEATURES** GENERATED FROM AAL TEMPLATE, NEUROMARK TEMPLATE AND MOO-ICAR

|                    | AAL      |          |                       | NeuroMark |          |                       | MOO-ICAR    |          |                       |
|--------------------|----------|----------|-----------------------|-----------|----------|-----------------------|-------------|----------|-----------------------|
|                    | <i>r</i> | <i>p</i> | <i>R</i> <sup>2</sup> | <i>r</i>  | <i>p</i> | <i>R</i> <sup>2</sup> | <i>r</i>    | <i>p</i> | <i>R</i> <sup>2</sup> |
| HAMD17             | 0.29     | 2.4e-5   | 0.06                  | 0.25      | 2.6e-4   | 0.07                  | <b>0.37</b> | 4.8e-8   | 0.13                  |
| HAMA               | 0.35     | 1.9e-7   | 0.11                  | 0.24      | 4.1e-4   | 0.09                  | <b>0.38</b> | 1.2e-8   | 0.14                  |
| Somatization       | 0.23     | 7.5e-4   | 0.02                  | 0.29      | 2.2e-5   | 0.03                  | 0.29        | 2.6e-5   | 0.03                  |
| Weight change      | 0.40     | 2.5e-9   | 0.09                  | 0.52      | 2.1e-15  | 0.10                  | 0.34        | 5.9e-7   | 0.09                  |
| cognitive disorder | 0.17     | 1.3e-2   | 0.02                  | 0.33      | 1.6e-6   | 0.06                  | 0.43        | 6.6e-11  | 0.17                  |
| Psycho-retardation | 0.27     | 7.1e-5   | 0.07                  | 0.32      | 2.9e-6   | 0.08                  | 0.37        | 6.7e-8   | 0.10                  |
| Sleep disorders    | 0.35     | 2.7e-7   | 0.11                  | 0.33      | 1.5e-6   | 0.06                  | 0.38        | 1.9e-8   | 0.10                  |
| HAMD-6             | 0.28     | 5.6e-5   | 0.05                  | 0.35      | 2.7e-7   | 0.10                  | 0.40        | 2.9e-9   | 0.14                  |

Anxiety/somatization: HAMD 10, 11, 12, 15, 17; Weight change: HAMD 16; Cognitive disturbance: HAMD 2, 3, 9; Psychomotor retardation: HAMD 1, 7, 8, 14; Sleep disturbance: HAMD 4, 5, 6; HAMD-6: HAMD 1, 2, 7, 8, 10, 13. MDD major depressive disorder, HCs health controls, HAMD-17 Hamilton depression scale-17, HAMA Hamilton anxiety scale. **Bold** values correspond to the highest correlation in HAMD17 and HAMA models.

#### IV. DISCUSSION

In this study, a novel approach—ICA-based IDSSN—was used to construct structural similarity networks at the individual level based on T1w images. The superiority of ICA-based IDSSN over using templates (AAL atlas, NeuroMark template) to construct structural similarity networks was that ICA-based IDSSN uses a data-driven approach that does not rely on any pre-defined brain atlas. It combines spatial priority information from ICA with morphological characteristics of brain regions from structural similarity network, which allows us to explore correlations between clinically meaningful indicators and structural similarity networks and identify unique neuroanatomical patterns of patients. It is worth noting that for new subjects, the model does not need to be retrained and can be directly applied for personalized analysis.

Based on a population of adolescent MDD patients, we obtained ICA-based IDSSNs that can quantify individual anxiety and depression symptoms, thus quantifying the brain structure of the subjects. The obtained individualized fingerprints could reflect individual differences and are related to individual development, and disease course. In addition, the experimental results also show that using templates to divide GMV to construct structural similarity matrices or only using extracted features without constructing structural similarity networks, the prediction accuracy of HAMD and HAMA scores is lower than that of features obtained from ICA-based IDSSN. Meanwhile, the prediction accuracy in six subdomains strongly confirms the conclusion that implying that ICA spatial priority information and structural similarity network information can reveal more specific information reflecting individual disease differences.

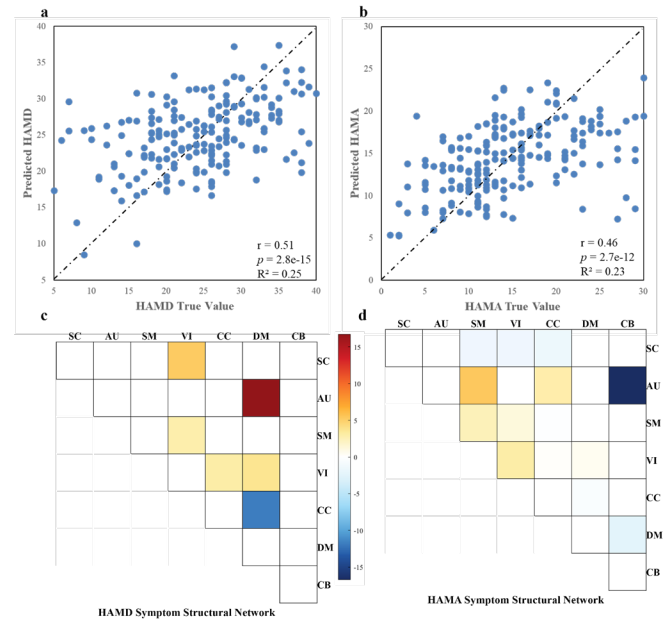


Figure 2. Scatter plot of the model-estimated symptom scores with respect to observed values using ICA-based individualized differential structure similarity networks (IDSSN) features, and distribution of the structural connections. When using IDSSN features as input for CPM, Pearson's correlations of  $r_{[HAMD17]} = 0.51$  ( $p = 2.8e-15$ ), and  $r_{[HAMA]} = 0.46$  ( $p = 2.7e-12$ ) between predicted and observed symptom scores were achieved for HAMD (a) and HAMA (b) respectively. The goodness of fit is measured by the degree to which the points are close to the dotted line in the plot (diagonal  $y = x$ ). Matrices present the contributions (right) and raw number of edges (left) for seven NeuroMark templates defined brain regions for the high-HAMD symptom (red) networks and low-HAMD symptom (blue) networks (c) and for the high-HAMA symptom (red) networks and low-HAMA symptom (blue) networks (d). The red to blue colorbar in c and d indicated edge contributions in every region. The darker red indicates higher involvement in the high-cognitive (red) network, while the darker blue indicates higher engagement in the low-cognitive (blue) network.

The brain is a complex network that supports information transfer, and structurally similar networks appear to reflect maturation or atrophy among brain regions. Our results suggest that depressive symptom in MDD is associated with changes in connectivity between the VI and other networks that are thought to be involved in the perception and processing of emotional facial expressions[10]. Abnormal networks were also observed in DM, CC, and SM, which are associated with emotion regulation and cognitive

function[11]. Interestingly, networks contributing to the prediction of anxiety symptoms in MDD are more widely involved than those associated with depressive symptoms and are found in VI, CC, SC, and CB, suggesting some anatomical differences in the causes of anxiety symptoms and depressive symptoms. Therefore, the ICA-based IDSSN can be used to measure the anatomical connectome of the brain and to make quantitative predictions of anxiety and depression in individuals.

Despite the innovative analytical approach and robust findings, the present study is subject to certain limitations. First, due to the relatively small sample size, predictive analyses were performed within the LOOCV framework, rather than utilizing the more stringent 5-fold or 10-fold cross-validation strategy. This may have increased the variance and instability of the prediction results. Therefore, future research should aim to construct models based on more stringent cross-validation strategies and use independent datasets to verify the generalization performance of the model. Another potential limitation is that this study is a cross-sectional study, and as such, there is no longitudinal sample to further verify the conclusions of this study. Therefore, a longitudinal analysis of a larger cohort of MDD patients is needed to verify the causal relationship between brain structural changes and clinical symptoms. It is worth noting that although this study used ICA-based IDSSN to predict clinical symptoms in adolescent patients with MDD, the disease-specific information provided by ICA-based IDSSN features can be generalized to the prediction of clinical symptoms and cognitive ability in other neurological or psychiatric disorders.

## V. CONCLUSION

In summary, the current study used an ICA-based approach to construct structural similarity networks in MDD patients and explored the correlation between ICA-based IDSSN and symptom manifestations of depression and anxiety. Results show that IDSSN features can provide supporting anatomical information for understanding complex mental disorders, especially for single new individual patient. Meanwhile, by integrating the spatial prior information of ICA and the structural similarity network, the extracted features are guaranteed to identify personalized GM fingerprints better than features based on the normal fixed brain atlas (AAL atlas, NeuroMark template). The present study, to some extent, remedies the lack of analysis of individual differences in morphological networks among MDD patients, and may facilitate the identification of imaging markers on the road to understanding the pathological basis of MDD. The current study offers a new approach that can enhance ability to detect GM deviations between certain individual patient and healthy groups, providing new insight on evaluating individual-level clinical heterogeneity based on brain structural features.

## REFERENCES

- [1] L. Schmaal *et al.*, "Cortical abnormalities in adults and adolescents with major depression based on brain scans from 20 cohorts worldwide in the ENIGMA Major Depressive Disorder Working Group," *Mol Psychiatry*, vol. 22, no. 6, pp. 900-909, 2017.
- [2] M.-Y. Du *et al.*, "Voxelwise meta-analysis of gray matter reduction in major depressive disorder," *Progress in Neuro-Psychopharmacology and Biological Psychiatry*, vol. 36, no. 1, pp. 11-16, 2012.
- [3] L. Schmaal *et al.*, "Cortical abnormalities in adults and adolescents with major depression based on brain scans from 20 cohorts worldwide in the ENIGMA Major Depressive Disorder Working Group," *Mol Psychiatry*, vol. 22, no. 6, pp. 900-909, 2017.
- [4] P. D. Harvey, D. Koren, A. Reichenberg, and C. R. Bowie, "Negative symptoms and cognitive deficits: what is the nature of their relationship?," *Schizophr Bull*, vol. 32, no. 2, pp. 250-8, 2006.
- [5] Z. Liu *et al.*, "Resolving heterogeneity in schizophrenia through a novel systems approach to brain structure: individualized structural covariance network analysis," *Mol Psychiatry*, vol. 26, no. 12, pp. 7719-7731, 2021.
- [6] K. Zhao *et al.*, "Regional Radiomics Similarity Networks Reveal Distinct Subtypes and Abnormality Patterns in Mild Cognitive Impairment," *Adv Sci*, vol. 9, no. 12, p. 2104538, 2022.
- [7] X. Shen *et al.*, "Using connectome-based predictive modeling to predict individual behavior from brain connectivity," *Nature Protocols*, vol. 12, no. 3, pp. 506-518, 2017.
- [8] X. Hu *et al.*, "Sex-specific alterations of cortical morphometry in treatment-naïve patients with major depressive disorder," *Neuropsychopharmacology : official publication of the American College of Neuropsychopharmacology*, vol. 47, no. 11, pp. 2002-2009, 2022.
- [9] Y. Du *et al.*, "NeuroMark: An automated and adaptive ICA based pipeline to identify reproducible fMRI markers of brain disorders," *Neuroimage Clin*, vol. 28, p. 102375, 2020.
- [10] X. Zhong *et al.*, "Whole-brain resting-state functional connectivity identified major depressive disorder: A multivariate pattern analysis in two independent samples," *J Affect Disord*, vol. 218, pp. 346-352, 2017.
- [11] P. C. Mulders, P. F. van Eijndhoven, A. H. Schene, C. F. Beckmann, and I. Tendolkar, "Resting-state functional connectivity in major depressive disorder: a review," *Neuroscience & Biobehavioral Reviews*, vol. 56, pp. 330-344, 2015.